

Data supplement for Scheele et al., Treatment-Resistant Depression and Ketamine Response in a Patient With Bilateral Amygdala Damagey. *Am J Psychiatry* (doi: 10.1176/appi.ajp.2019.18101219)

SUPPLEMENTAL METHODS

Participants

The study was approved by the local ethics committee of the Medical Faculty of the University of Bonn, Germany. All participants gave written informed consent and the study was conducted in accordance with the latest revision of the Helsinki Declaration. The 12 control patients with major depressive disorder (MDD) received inpatient treatment at the University Hospital Bonn and were treated according to current guidelines. The treatment included psychotherapy and antidepressant medication. All MDD patients were scanned within three days after admission (mean age \pm SD = 42.75 \pm 13.23 years; mean MADRS score \pm SD = 28.00 \pm 6.61). Furthermore, to examine possible structural changes in the MDD patients, structural images of 16 healthy women (mean age \pm SD = 39.88 \pm 11.79 years; mean BDI score \pm SD = 1.31 \pm 1.53) were used that were collected on the same MRI system.

Screening questionnaires

Loneliness was assessed with the UCLA Loneliness Scale (1) and the Social Network Index (SNI) questionnaire was used to examine the patient's social network (2). Depressive symptoms were measured with the Beck Depression Inventory-II (BDI)(3) and the Montgomery-Åsberg Depression Rating Scale (MADRS)(4). Suicidal ideation was assessed with the Columbia-Suicide Severity Rating Scale (C-SSRS)(5). Dissociative symptoms were evaluated with the Clinician-Administered Dissociative States Scale (CADSS)(6). Psychological disorders were assessed with a Structured Clinical Interview for DSM-IV (7) conducted by an experienced psychiatrist who was familiar with the patient's medical history.

Acquisition of the MRI data

The MRI data were collected using a 1.5-tesla Siemens Avanto MRI system (Siemens AG, Erlangen, Germany) equipped with a 12-channel head-coil. T2*-weighted echoplanar (EPI) images with blood-oxygen-level dependent contrast were obtained [repetition time (TR) = 3070 ms, echo time (TE) = 45 ms, interleaved slicing, matrix size: 64 x 64, voxel size: 3 x 3 x 3 mm, FoV = 192 mm, flip angle 90°, 38 axial slices]. The duration of each resting state session was 6 minutes. In addition, high-resolution anatomical images were acquired on the same scanner using a T1-weighted 3D MPRAGE sequence (imaging parameters: TR = 1660 ms, TE = 3.09 ms, matrix size: 256x256, voxel size: 1 x 1 x 1 mm, FoV = 256 mm, flip angle 15°, 160 sagittal slices).

Anatomical images of the amygdala patient were also acquired on a 3.0-tesla Siemens TRIO MRI system (Siemens AG, Erlangen, Germany), using a T1-weighted 3D MPRAGE sequence (imaging parameters: TR = 1660 ms, TE = 2.54 ms, matrix size: 320x320, voxel size: 0.8 x 0.8 x 0.8 mm, flip angle 9°, 208 sagittal slices).

fMRI data analysis

Analysis of resting state functional magnetic resonance imaging (rsfMRI) data was performed using the CONN toolbox, version 18a (<https://web.conn-toolbox.org/>; (8)), and statistical parametric mapping, version 12 (<http://www.fil.ion.ucl.ac.uk/spm/software/spm12>), implemented in MATLAB R2018a

(MathWorks, Natick, Massachusetts). The first five volumes were discarded to allow MRI T1 equilibration. Preprocessing of the remaining volumes was done using CONN's standard pipeline including realignment, coregistration with a high-resolution anatomic scan, slice-time correction, structural segmentation, normalization to Montreal Neurological Institute standard brain template, and spatial smoothing (Gaussian kernel of 6 mm³ full-width at half maximum). After the preprocessing steps, data were denoised using the anatomical component-based noise correction (aCompCor) (9) method. White matter and cerebrospinal fluid time series along with the effect rest (rest condition convolved with hemodynamic response function) were regressed out. A band-pass filter (0.008–0.09 Hz) and detrending (removal of linear trends within each functional session) were applied to the time series to reduce low-frequency drift and noise effects. We used the masks provided within CONN as seeds for the default mode network (DMN) (medial prefrontal cortex MNI coordinates x, y, z: 1, 55, -3; posterior cingulate cortex MNI coordinates x, y, z: 1, -61, 38; left lateral parietal cortex MNI coordinates x, y, z: -39, -77, 33; and right lateral parietal cortex MNI coordinates x, y, z: 47, -67, 29), frontoparietal network (FPN) (left prefrontal cortex MNI coordinates x, y, z: -43, 33, 28; right prefrontal cortex MNI coordinates x, y, z: 41, 38, 30; left posterior parietal cortex MNI coordinates x, y, z: -46, -58, 49; right posterior parietal cortex MNI coordinates x, y, z: 52, -52, 45) and salience network (SAN) (anterior cingulate cortex MNI coordinates x, y, z: 0, 22, 35; left anterior insula MNI coordinates x, y, z: -44, 13, 1; right anterior insula MNI coordinates x, y, z: 47, 14, 0; left rostral prefrontal cortex MNI coordinates x, y, z: -32, 45, 27; right rostral prefrontal cortex MNI coordinates x, y, z: 32, 46, 27; left supramarginal gyrus MNI coordinates x, y, z: -60, -39, 31; right supramarginal gyrus MNI coordinates x, y, z: 62, -35, 32). Correlation coefficients were converted to normalized z-scores using Fisher's transformation to allow subsequent general linear model analyses. Seed-to-voxel analysis was performed at an individual-subject level in CONN by computing BOLD signal temporal correlations between the previously mentioned seeds and all other voxels in the brain. First, we computed a separate analysis of variance (ANOVA) for each seed region in which we tested any difference between the patient's four resting state measurements and the MDD controls. To evaluate differences between repeated measurements of patient AM, the MDD controls were modeled as 0 to obtain the necessary variance for a second-level analysis. In case of significant differences, we used independent *t*-tests to separately compare each resting state measurement of the patient with the MDD controls. All analyses applied a height threshold of $P < 0.001$ (uncorrected) at the whole-brain level. *P*-values were corrected for multiple comparisons (false discovery rate (FDR)) and $P_{\text{FDR}} < 0.05$ was considered significant. The structural images and contrast images of the resting state data were uploaded to a public repository (<https://neurovault.org/collections/RDWCTHVB/>).

Voxel-Based Morphometry

The CAT12 toolbox (Computational Anatomy Toolbox 12, Structural Brain Mapping group, Jena University Hospital, Jena, Germany) implemented in SPM12 was used with default settings for the preprocessing of the structural images. All T1-weighted images were corrected for bias-field inhomogeneities, tissue classified and spatially normalized to MNI-space at a voxel size of $1.5 \times 1.5 \times 1.5$ mm³ using the diffeomorphic anatomical registration through exponentiated lie algebra (DARTEL) algorithm (10). Homogeneity of gray matter images was checked using the covariance structure of each image with all other images, as implemented in the check data quality function. In addition to visual inspections, all scans passed the automated data quality check protocol. Subsequently, the modulated gray matter volume (referred to as GMV) images were smoothed with an isotropic Gaussian kernel of 6 mm full width half maximum (FWHM). The GMV data were analyzed using an absolute threshold masking of 0.1. The amygdala was anatomically defined according to the Wake Forest University Pick Atlas (Version 3.0) and GMV values were extracted from the amygdala using the `get_totals` script (<http://www.nemotos.net/?p=292>).

SUPPLEMENTAL RESULTS

Resting state data

Default mode network

We first tested whether there were any significant differences between the patient's measurements and the MDD controls. We detected significantly altered connectivity between the posterior cingulate cortex as seed and the left frontal pole (-10, 64, 18; $k = 20$, $F_{(4,11)} = 27.47$, $P_{FDR} = 0.05$; -24, 44, 40; $k = 18$, $F_{(4,11)} = 21.83$, $P_{FDR} = 0.05$). Separate comparisons of the patient's measurements and the MDD controls revealed significantly enhanced positive connectivity between the posterior cingulate cortex and the frontal pole 200 minutes after the first infusion (-10, 64, 18; $k = 70$, $t_{(11)} = 10.22$, $P_{FDR} < 0.01$) and one day after the infusion (32, 44, 38; $k = 53$, $t_{(11)} = 6.77$, $P_{FDR} < 0.01$). We also found a significant change in the correlation between the posterior cingulate cortex and the signal in the left cerebellum (negative correlation in the patient and positive correlations in the MDD controls) 200 minutes after the infusion (-40, -60, -42; $k = 41$, $t_{(11)} = 6.27$, $P_{FDR} = 0.05$).

Furthermore, we found significantly altered DMN connectivity between the right lateral parietal cortex as seed and the left frontal pole (-14, 66, 4; $k = 22$, $F_{(4,11)} = 24.74$, $P_{FDR} = 0.02$) and the left cerebellum (-36, -64, -44; $k = 22$, $F_{(4,11)} = 52.59$, $P_{FDR} = 0.02$). Separate comparisons of the patient's measurements and the MDD controls revealed significantly enhanced positive connectivity between the right lateral parietal cortex and the frontal pole 200 minutes after the first infusion (-12, 66, 4; $k = 80$, $t_{(11)} = 8.95$, $P_{FDR} < 0.01$).

Significant differences were also evident in the functional coupling between the medial prefrontal cortex as seed and the superior frontal gyrus (12, -6, 76; $k = 26$, $F_{(4,11)} = 27.56$, $P_{FDR} = 0.02$), the precuneus (4, -68, 18; $k = 21$, $F_{(4,11)} = 27.81$, $P_{FDR} = 0.02$) and the left cerebellum (-38, -72, -40; $k = 23$, $F_{(4,11)} = 19.92$, $P_{FDR} = 0.02$). Separate comparisons of the patient's measurements and the MDD controls revealed significantly enhanced positive connectivity between the medial prefrontal cortex as seed and the superior frontal gyrus (12, -6, 76; $k = 78$, $t_{(11)} = 9.83$, $P_{FDR} < 0.01$) at baseline and the frontal pole (-8, 70, 2; $k = 58$, $t_{(11)} = 6.92$, $P_{FDR} < 0.01$), the precuneus (2, -54, 44; $k = 109$, $t_{(11)} = 6.91$, $P_{FDR} < 0.01$), the lateral occipital cortex (40, -74, 48; $k = 46$, $t_{(11)} = 8.56$, $P_{FDR} < 0.01$), and the occipital pole (28, -92, 20; $k = 50$, $t_{(11)} = 5.85$, $P_{FDR} < 0.01$) in the patient 200 minutes after the first infusion. There was also a trend-to-significant effect on the connectivity with the frontal pole one day after the first infusion (30, 40, 34; $k = 34$, $t_{(11)} = 5.65$, $P_{FDR} = 0.079$). In addition, we observed negative correlations between the medial prefrontal cortex and the left cerebellum (-40, -68, -44; $k = 41$, $t_{(11)} = 7.57$, $P_{FDR} = 0.02$), the middle temporal gyrus (60, -52, -4; $k = 48$, $t_{(11)} = 7.32$, $P_{FDR} = 0.02$), the precuneus (4, -56, 14; $k = 46$, $t_{(11)} = 6.02$, $P_{FDR} = 0.02$), and the right superior parietal lobule (36, -40, 54; $k = 35$, $t_{(11)} = 6.21$, $P_{FDR} = 0.03$) in the patient 200 minutes after the first infusion compared to positive correlations in the MDD controls. The negative correlation between the medial prefrontal cortex and precuneus was also evident in the patient seven days after the infusion (4, -68, 18; $k = 65$, $t_{(11)} = 7.03$, $P_{FDR} < 0.01$).

Frontoparietal network

We first tested whether there were any significant differences between the patient's measurements and the MDD controls. We detected significantly altered connectivity between the right posterior parietal cortex as seed and the left superior frontal gyrus and frontal pole (-8, 32, 58; $k = 31$, $F_{(4,11)} = 16.47$, $P_{FDR} < 0.01$), the middle temporal gyrus (70, -40, -2; $k = 19$, $F_{(4,11)} = 29.18$, $P_{FDR} = 0.05$) and the right cerebellum (38, -70, -50; $k = 18$, $F_{(4,11)} = 44.56$, $P_{FDR} = 0.05$). There were no significant differences for other seeds of the frontoparietal network. Separate comparisons of the patient's measurements and the MDD controls revealed significantly enhanced positive connectivity between the right posterior parietal cortex and the superior frontal gyrus and frontal pole (-12, 36, 60; $k = 81$, $t_{(11)} = 6.67$, $P_{FDR} < 0.01$) and the right lateral occipital cortex (42, -90, 4; $k = 52$, $t_{(11)} = 6.28$, $P_{FDR} = 0.01$) 200 minutes after the first infusion. Furthermore, there was a significantly enhanced positive correlation between the right posterior parietal cortex as seed and the left occipital pole (-34, -96, -2; $k = 46$, $t_{(11)} = 5.82$, $P_{FDR} = 0.05$) one day after the infusion and with the right middle temporal gyrus (70, -40, -2; $k = 48$, $t_{(11)} = 5.82$, $P_{FDR} = 0.03$) seven days after the infusion.

Salience network

We first tested whether there were any significant differences between the patient's measurements and the MDD controls. We detected significantly altered connectivity between the anterior cingulate cortex as seed and the frontal pole (-42, 42, 14; $k = 20$, $F_{(4,11)} = 29.26$, $P_{\text{FDR}} = 0.03$) and the precuneus (-4, -56, 34; $k = 26$, $F_{(4,11)} = 16.35$, $P_{\text{FDR}} = 0.02$). There were no significant differences for other seeds of the salience network. Separate comparisons of the patient's measurements and the MDD controls revealed significantly enhanced positive connectivity between the anterior cingulate cortex and the precuneus (-4, -56, 34; $k = 60$, $t_{(11)} = 6.63$, $P_{\text{FDR}} < 0.01$) at baseline. There were no significant differences 200 minutes and one day after the first infusion, but the significantly altered connectivity with the precuneus was again evident after seven days (-2, -60, 32; $k = 39$, $t_{(11)} = 5.12$, $P_{\text{FDR}} = 0.06$).

Second ketamine infusion

A second ketamine infusion with a reduced dose (0.25 mg/kg) was administered seven days after the first ketamine infusion to examine if a similar antidepressant effect could be achieved, while reducing the dissociative symptoms after the infusion. The ketamine-induced dissociative symptoms were diminished compared to the first infusion (50 minutes after the first infusion CADSS = 24; 50 minutes after the second infusion CADSS = 17) and vanished after 130 minutes (first infusion CADSS = 2; second infusion CADSS = 0). However, the antidepressant effect was also less pronounced (59% reduction of the MADRS score 50 minutes after infusion; cf. **Supplementary Figure 1**) relative to the first infusion with a ketamine dose of 0.5 mg/kg. Depressive symptoms returned to baseline after two days. This observation is in accordance with a recent dose-ranging trial of intravenous ketamine that found clear evidence for clinically meaningful efficacy only for the standard dose (0.5 mg/kg) and high dose (1 mg/kg) of intravenous ketamine (11). Ms. M. was discharged at her own request two weeks after the second ketamine infusion.

Venous blood samples were collected 50 minutes after the first and second ketamine infusions to measure serum concentrations of ketamine and norketamine (the active metabolite of ketamine). As expected, the second infusion yielded lower concentrations (ketamine = 40 $\mu\text{g/l}$, norketamine = 30 $\mu\text{g/l}$) compared to the first infusion with the higher dose (ketamine = 149 $\mu\text{g/l}$, norketamine = 35 $\mu\text{g/l}$).

Additional ratings

The Hamilton Rating Scale for Depression (HAM-D) (12) was administered six times: before, one day after and seven days after the first and second ketamine infusion. There was a clear reduction of HAM-D scores after the first ketamine infusion (0.5 mg/kg) (before infusion = 31, one day after infusion = 16, seven days after infusion = 23), but only a small effect was evident one day after the second ketamine infusion with a lower dose of 0.25 mg/kg (before infusion = 25; one day after infusion = 23; seven days after infusion = 25). Two items of the HAM-D assess psychological and somatic anxiety symptoms. Consistent with the clinical phenotype of Urbach Wiethe disease, the patient showed only low levels of anxiety (sum score anxiety items = 3; possible maximum 8) at baseline and these symptoms decreased after the first ketamine infusion (one day after infusion sum score anxiety items = 0; seven days after infusion sum score anxiety items = 1).

VBM results

The total GMV ($t_{(26)} = 0.91$, $P = 0.37$) and the GMV of the left ($t_{(26)} = 1.25$, $P = 0.22$) and right amygdala ($t_{(26)} = 0.60$, $P = 0.55$) were not significantly different between MDD patients and healthy controls. Thus, it seems unlikely that MDD-associated structural changes in the amygdala volume of the MDD controls have contributed to the observed difference in functional connectivity.

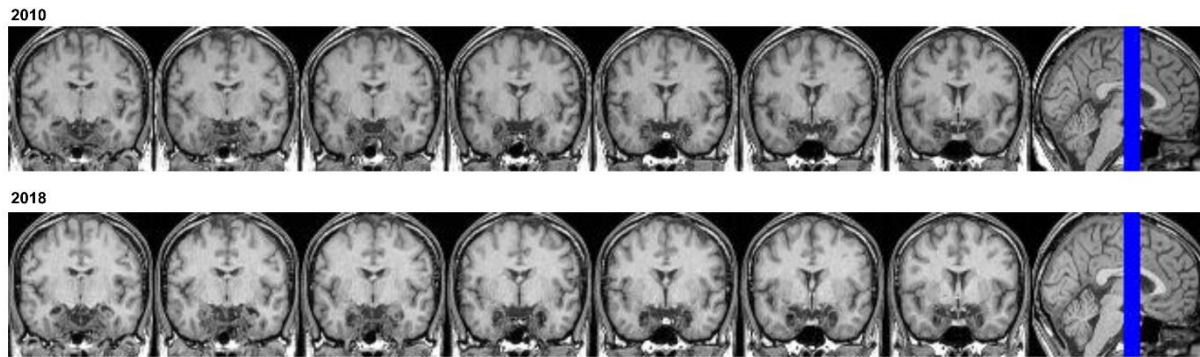
Supplemental Tables and Figures

TABLE S1. Failed antidepressant treatments in the amygdala patient

Treatment	Dose
Atypical antipsychotics with antidepressant action	
Quetiapine	100 mg/day
Olanzapine	5 mg/day
Cognitive-behavioral therapy (CBT)	1 session/week
Electroconvulsive therapy (ECT)	
Unilateral ECT	12 sessions
Bilateral ECT	15 sessions
Monoamine oxidase inhibitors (MAOIs)	
Tranylcypromine	20 mg/day
Norepinephrine and dopamine disinhibitors (NDDIs)	
Bupropione	150 mg/day
Other antidepressants	
Agomelatine	25-50 mg/day
Mirtazapine	30-60 mg/day
Tianeptine	37.5 mg/day
Selective serotonin reuptake inhibitors (SSRIs) and serotonin modulators	
Citalopram	10-40 mg/day
Sertraline	100 mg/day
Vortioxetine	10-15 mg/day
Selective serotonin and norepinephrine reuptake inhibitors (SSNRI)	
Duloxetine	30-120 mg/day
Venlafaxine	150 mg/day
Tricyclics (TCAs) and heterocyclics	
Trimipramine	150 mg/day

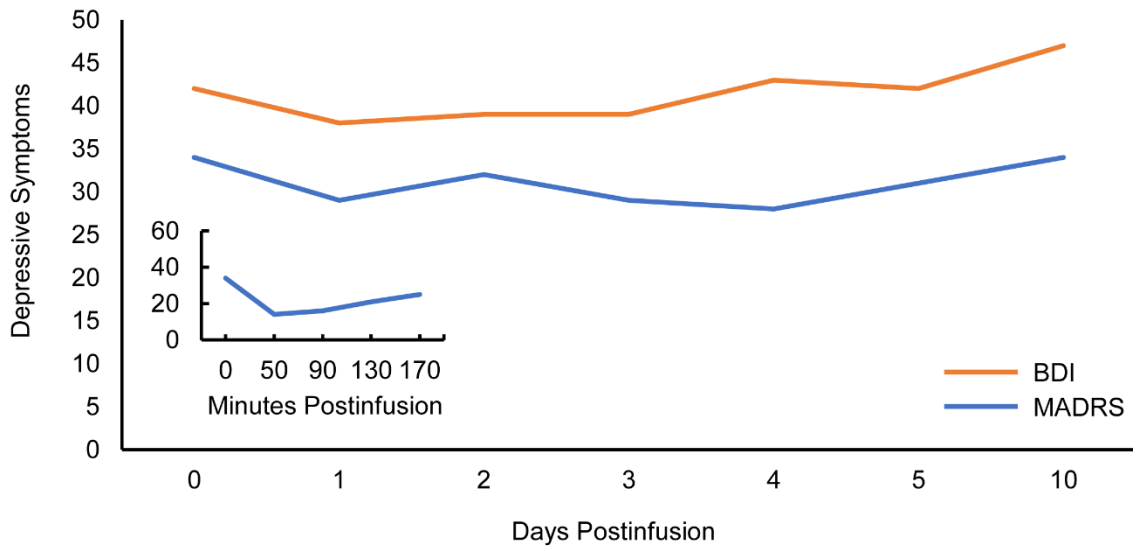
Note: Several medications were prescribed in parallel. The duration of treatments varied over the course of three years (2015-2018), but the minimum durations were in accordance with current guidelines (13).

FIGURE S1.



Normalized coronal anatomical T1-weighted magnetic resonance images of patient AM's amygdala lesion in the years 2010 and 2018. Anatomical inspection of patient AM's scans reveals complete bilateral destruction of the basolateral amygdala with minor sparing in anterior amygdaloid and ventral cortical amygdaloid regions at a rostral level and central amygdaloid nucleus and the amygdalo-hippocampal transition zone at more caudal levels. Notably, her lesion has remained stable over this time period and has not progressed into other regions of the brain.

FIGURE S2.



Depressive symptoms were assessed for five consecutive days and 10 days after a second subanesthetic i.v. dose (0.25 mg/kg) of ketamine in a patient with severe depression despite bilateral amygdala damage. Clinician-evaluated depressive symptoms were reduced after the ketamine infusion, but the magnitude of this antidepressant effect was smaller than the effect observed after the first infusion with a large ketamine dose (0.5 mg/kg). The inlay display changes in the clinician-rated depressive symptoms in the 170 minutes after the ketamine infusion.

Supplemental References

1. Russell DW: UCLA Loneliness Scale (Version 3): reliability, validity, and factor structure. *J Pers Assess* 1996; 66:20-40
2. Cohen S, Doyle WJ, Skoner DP, Rabin BS, Gwaltney JM, Jr.: Social ties and susceptibility to the common cold. *JAMA* 1997; 277:1940-1944
3. Beck AT, Steer RA, Brown GK: Beck depression inventory-II. San Antonio, TX: Psychological Corporation; 1996
4. Montgomery SA, Asberg M: A new depression scale designed to be sensitive to change. *Br J Psychiatry* 1979; 134:382-389
5. Posner K, Brown GK, Stanley B, Brent DA, Yershova KV, Oquendo MA, et al: The Columbia-Suicide Severity Rating Scale: initial validity and internal consistency findings from three multisite studies with adolescents and adults. *Am J Psychiatry* 2011; 168:1266-1277
6. Bremner JD, Krystal JH, Putnam FW, Southwick SM, Marmar C, Charney DS, et al: Measurement of dissociative states with the Clinician-Administered Dissociative States Scale (CADSS). *J Trauma Stress* 1998; 11:125-136
7. Wittchen H, Wunderlich U, Gruschwitz S, Zaudig M: Strukturiertes Klinisches Interview für DSM-IV [Structured clinical interview for DSM-IV]. Goettingen, Hogrefe; 1997
8. Whitfield-Gabrieli S, Nieto-Castanon A: Conn: a functional connectivity toolbox for correlated and anticorrelated brain networks. *Brain Connect* 2012; 2:125-141
9. Muschelli J, Nebel MB, Caffo BS, Barber AD, Pekar JJ, Mostofsky SH: Reduction of motion-related artifacts in resting state fMRI using aCompCor. *Neuroimage* 2014; 96:22-35
10. Ashburner J: A fast diffeomorphic image registration algorithm. *Neuroimage* 2007; 38:95-113
11. Fava M, Freeman MP, Flynn M, Judge H, Hoepfner BB, Cusin C, et al: Double-blind, placebo-controlled, dose-ranging trial of intravenous ketamine as adjunctive therapy in treatment-resistant depression (TRD). *Mol Psychiatry* 2018;
12. Hamilton M: A rating scale for depression. *J Neurol Neurosurg Psychiatry* 1960; 23:56-62
13. DGPPN, BÄK, KBV, AWMF, AkdÄ, BPTK, BApK, DAGSHG, DEGAM, DGPM, DGPs, DGRW (Editors) for the Guideline Group Unipolar Depression: S3-Guideline/National Disease Management Guideline Unipolar Depression. Short Version 2009. Berlin, Düsseldorf: DGPPN, ÄZQ, AWMF; 2009